

Dipole-dipole collision-induced transport of resonance excitation in a high-density atomic vapor

H. van Kampen, V. A. Sautenkov, A. M. Shalagin,* E. R. Eliel, and J. P. Woerdman
Huygens Laboratory, Leiden University, P.O. Box 9504, 2300 RA Leiden, The Netherlands

(Received 6 June 1997)

We have experimentally studied the nonradiative transport of excitation in a dense [$N=(0.3-2.5)\times 10^{17}\text{ cm}^{-3}$] potassium vapor. We show that in such a high-density vapor the diffusive nonradiative transport of excitation via ‘‘hopping’’ of excitation in dipole-dipole collisions between excited- and ground-state atoms is dominant over the radiative transport through photons. The nonradiative transport mechanism becomes visible in the fluorescence-excitation spectrum signal as a sharp dip close to the resonance frequency. The appearance of the dip, its shape, width, and density dependence can all be explained in terms of a simple diffusion model for the nonradiative transport. This yields values for the diffusion coefficient and the resonance-exchange rate coefficient. [S1050-2947(97)03611-1]

PACS number(s): 32.70.Jz, 32.50.+d

I. INTRODUCTION

It is well known that the interatomic interaction in a high-density atomic vapor where part of the atoms is in the first excited state is dominated by the resonant dipole-dipole interaction between ground- and excited-state atoms. Because of the long-range nature of the resonant dipole-dipole interaction each atom interacts not only with close neighbors but also with atoms that are far away. One can approximate the effect of the nearby atoms by invoking line-broadening theory. The dipole-dipole collisions give rise to a self-broadened atomic response having a Lorentzian shape with a width Γ_{self} . In the binary-collision limit Γ_{self} is proportional to density N and one writes $\Gamma_{\text{self}}=\langle\sigma v\rangle N$ with σ the cross section for dipole-dipole collisions and v the relative speed of the atoms. The average is performed over the relative velocities of the collision partners.

The effect of the far-removed atoms can be taken into account in a mean-field sense using a local-field model, or equivalently, the Clausius-Mosotti relations [1]. Here one assumes that the local field rather than the external optical field governs the atomic response [2,3], where the local field is the field due to both the external light source and all the other atoms in the gas. In the linear optical response approximation the local field gives rise to the Lorentz shift, a density- and excitation-dependent shift of the atomic resonance frequency [4,5]. Because of the excitation dependence of this shift there has been considerable interest, recently, in local field effects, especially regarding nonlinear optical phenomena such as lasers without inversion [6], optical bistability [7,8], self-induced transparency [9], and piezophotonic switching [6].

A description in terms of optical response does not, however, do justice to the complex processes that arise in such a vapor. For instance, the spontaneous emission by the excited atoms is totally ignored. As a result of the high density of the vapor the spontaneously emitted photons travel only short distances before being reabsorbed by another atom. Since the

absorption probability depends on the detuning from resonance, this distance is determined by the frequency of the photon. After a spontaneous lifetime an atom that has absorbed the photon emits a new photon. This photon may have a totally different frequency (within the spectral line) as compared to that of the absorbed photon as a consequence of the collisions (collisional redistribution). In the end of the photons escape from the vapor because of its finite extent. This extensively studied process is known as radiation trapping. It is not possible to associate a mean free path with radiation trapping because one cannot define a single absorption length [10–12]. Note that in this process atoms exchange real photons.

Additionally, the atoms in the vapor can exchange excitation by nature of the dipole-dipole interaction; this process, where the excitation ‘‘hops’’ from an excited-state atom to a ground-state atom, corresponds to the exchange of a virtual photon [13]. Since the atoms are moving the excitation wanders through the vapor. With this nonradiative process one can associate a mean free path $l_{\text{re}}=v_{\text{th}}(\langle\sigma_{\text{re}}v\rangle N)^{-1}$, with σ_{re} the cross section for the resonance exchange process and v_{th} the most probable speed of an atom in the vapor. If l_{re} is much smaller than the thickness of the layer of excited atoms (this layer is usually thin due to the optical thickness of the vapor), the nonradiative transport of excitation is in principle of a diffusive nature. This condition is typically fulfilled in a sufficiently dense atomic vapor, i.e., a vapor for which the self-broadened linewidth is much larger than the Doppler width.

In treatments of radiative transport in gases the nonradiative contribution has long been ignored; instead one has usually solved the incomplete transport equation, only including radiation trapping [10,14]. In most cases these treatments gave satisfactory agreement with experimental results. The fact that one also has to include nonradiative transport was first demonstrated in experiments by Phelps and co-workers [15–17]. They excited an atomic vapor through a window and measured the backscattered fluorescence. In this way a fluorescence-excitation spectrum of the vapor was obtained that showed a dip around line center that was attributed to the nonradiative contribution to the transport of excitation. In their experiment, however, the density ($N\approx 10^{14}\text{ cm}^{-3}$) was

*Present address: Institute of Automation and Electrometry, 630090 Novosibirsk, Russia.

such that l_{re} was roughly equal to the thickness of the excited layer, in contrast to the present experiment. Therefore, a quantitative description of their results in terms of a diffusion model is somewhat questionable.

The presence of the dip is caused by the cell window where excited atoms can lose their excitation nonradiatively (quenching). Whether the nonradiative contribution to the transport of excitation results in an observable reduction of the fluorescence yield is determined by the fraction of excited atoms that is sufficiently close to the cell wall. This in turn is determined by the relative order of three length scales: The absorption length l_a of the incoming light, the mean free path for resonance exchange l_{re} , and the diffusion length l_τ , which is the maximum distance the diffusive process of resonance exchange can cover within a spontaneous lifetime τ . $l_\tau = (\frac{1}{2}v_{\text{th}}l_{\text{re}}\tau)^{1/2}$. For a sufficiently dense atomic vapor excited at line center, the absorption length of the incoming light $l_a \approx \lambda/2\pi$; away from line center l_a increases proportionally to $(2\Delta\omega/\Gamma_{\text{self}})^2 + 1$, where $\Delta\omega$ is the detuning from line center and Γ_{self} the self-broadened full width at half maximum linewidth. The mean free path for resonance exchange $l_{\text{re}} \propto N^{-1}$.

When a vapor much denser than that investigated by Phelps and co-workers [15–17], e.g., $N \approx 10^{17} \text{ cm}^{-3}$, is excited at its resonance frequency we have $l_{\text{re}} \ll l_a < l_\tau$, meaning that the probability that an excited atom reaches the cell wall within the spontaneous lifetime and gets quenched is almost unity. In the meantime it has made many resonance-exchange collisions. The excitation transport is therefore dominantly nonradiative and diffusive in this case. The total fluorescent yield is small and, since the nonradiative transport occurs in a time short compared to the natural lifetime τ , the excitation is observed to decay also in a time short compared to τ . The latter effect has been corroborated in four-wave-mixing experiments [18].

When, however, the incident laser light is tuned to the wing of the spectral line, we have $l_{\text{re}} \ll l_\tau < l_a$; this means that the fraction of excited atoms that can reach the cell wall through diffusion, within the spontaneous lifetime τ , is small. Now the radiative transport dominates and the fluorescence yield is high. Note that we only consider the linear regime; i.e., the number of excited atoms is small as compared to the total number of atoms.

At extremely high densities, e.g., $N \approx 10^{20} \text{ cm}^{-3}$, three orders of magnitude higher than we consider in our experiment, the limit $l_{\text{re}} \ll l_\tau < l_a$ also applies for a vapor excited at line center. This situation can occur as a consequence of the density dependence of l_τ and the density independence of l_a at high densities.

In this paper we present a study of the transport of excitation in a high-density vapor ($N \approx 10^{17} \text{ cm}^{-3}$) under conditions where diffusion of excitation through nonradiative resonance-exchange collisions is dominant. We have been able to probe the purely diffusive limit in contrast to the experiment performed by Zajonc and Phelps [16] since we use much higher atomic densities. We will compare our experimental results with a diffusion model for the nonradiative transport and obtain values for the diffusion coefficient of the excitation and the resonance-exchange rate coefficient.

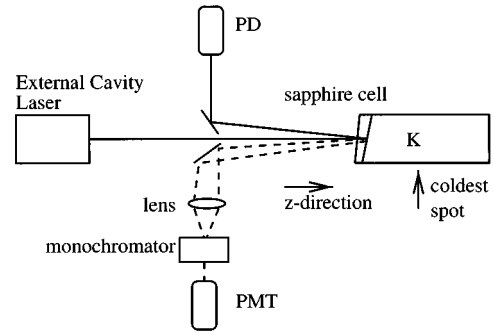


FIG. 1. Experimental setup to measure the fluorescence-excitation and the selective-reflection spectrum of a high-density potassium vapor.

II. EXPERIMENTAL TECHNIQUE

The experiments are performed using a continuously tunable, single-frequency, diode laser with an external cavity (New Focus model 6224), tuned to the D_1 transition of potassium ($\lambda = 770 \text{ nm}$). We use 4 mW of output power in a beam of a few mm diameter resulting in an intensity well below the saturating value ($\approx 1 \text{ W/cm}^2$ at a density $N = 0.2 \times 10^{17} \text{ cm}^{-3}$ [5]). The laser light is incident on an all-sapphire cell that contains the potassium vapor (see Fig. 1). The laser beam is reflected from the wedged entrance window of the cell so the reflections from the air-sapphire and sapphire-vapor interfaces can easily be distinguished. As a function of the frequency of the incident laser beam we measure the reflected beam and the backscattered fluorescence from the vapor with a silicon photodiode (PD) and a photomultiplier (PMT), respectively. The photomultiplier signal results in a fluorescence-excitation spectrum whereas the signal on the photodiode results in a selective-reflection spectrum [19].

We work with densities between 0.3 and $2.5 \times 10^{17} \text{ cm}^{-3}$, the density being determined by the temperature of the coldest spot of the cell (Fig. 1). This density is typically three orders of magnitude larger than that used by Zajonc and Phelps [16]. To avoid condensation of potassium vapor at the window its temperature is about 10 K higher than the cold spot. In the density range of interest the absorption length l_a is of the order of 10^{-7} m for light tuned near resonance. From the self-broadening coefficient for the D_1 line, $k = \Gamma_{\text{self}}/N = \langle \sigma v \rangle = 2\pi \times 5.9 \times 10^{-8} \text{ cm}^3 \text{ s}^{-1}$ [25], and simple theoretical considerations that relate k and $\langle \sigma_{\text{re}} v \rangle$ [16] we find $\langle \sigma_{\text{re}} v \rangle = 2\pi \times 3 \times 10^{-8} \text{ cm}^3 \text{ s}^{-1}$; here Γ_{self} represents the full width at half maximum of the spectral line. The value for the mean free path for resonance exchange l_{re} ranges then from 10^{-7} to 10^{-8} m , indeed smaller than l_a . Although l_{re} is only marginally smaller than l_a at the low side of the range of densities studied, a diffusive model for the nonradiative transport will prove to work surprisingly well.

Potassium is well suited for this study for the following reasons: the hyperfine splittings in the ground $4s^2S_{1/2}$ and excited $4p^2P_{1/2,3/2}$ states are relatively small ($< 0.5 \text{ GHz}$). In the density range of interest ($N = 0.3 - 2.5 \times 10^{17} \text{ cm}^{-3}$) the self-broadened width k of the resonance line is appreciably larger than the hyperfine splitting and the Doppler width (1 GHz at 600 K). Therefore we can ignore these effects. The

fine-structure splitting between the $^2P_{1/2}$ and $^2P_{3/2}$ states is large (1700 GHz), which would require one to take into account both excited levels. However, at the densities used, the fine-structure changing collisions are very frequent [20]; on average there is a fine-structure changing collision every 10 ns at $N=6 \times 10^{16} \text{ cm}^{-3}$. As a result, the $^2P_{3/2}$ state, which is not directly populated by the incident laser field, will be populated according to its statistical weight. This population mixing justifies the use of a two-level model for a discussion of our results; for the relevant parameters we consider an average of the values for the $^2P_{1/2}$ and $^2P_{3/2}$ states.

III. THEORETICAL MODEL

The distribution of excited atoms in a dense gas is governed by a transport equation containing terms that describe both radiative and nonradiative transport of excitation. The model presented in this section is based on earlier theoretical work [15,16,21]. For a system of two-level atoms located between infinite, parallel, plane boundaries the equation for the temporal variation of the spatial distribution $n(z,t)$ of excited atoms, with n much smaller than the total number of atoms, is given by

$$\frac{\partial n(z,t)}{\partial t} = -\gamma n(z,t) + D \frac{\partial^2}{\partial z^2} n(z,t) + \gamma \int G(z,z') n(z',t) dz' + S(z). \quad (1)$$

The first term on the right-hand side represents the loss of excited atoms due to spontaneous decay with rate $\gamma = \tau^{-1}$. The second term represents the diffusion of the excited atoms. Assuming only binary collisions between ground- and excited-state atoms the diffusion coefficient D can be written as

$$D = \frac{v_{\text{th}}^2}{2\nu_{\text{re}}}, \quad (2)$$

with $v_{\text{th}} = \sqrt{2k_B T/m}$, the thermal speed of the atoms (k_B is Boltzmann's constant, T the temperature of the vapor, and m the atomic mass). The frequency ν_{re} of resonance-exchange collisions is related to the resonance-exchange cross section σ_{re} by $\nu_{\text{re}} = \langle \sigma_{\text{re}} v \rangle N$ with N the density of the vapor. The brackets indicate an average over the relative velocity of the collision partners. The third term describes the radiation-trapping process [10] with a kernel $G(z,z')$ representing the probability that a photon emitted at z' is reabsorbed at z . The last term reflects the production of excited-state atoms. Steady-state solutions of this model have been discussed by Molisch *et al.* [21] in terms of a linear combination of solutions for the case where only radiative transport plays a role and the case where excitation hopping dominates.

As discussed earlier, at line center, the excitation transport is mainly determined by hopping of excitation via dipole-dipole collisions between ground- and excited-state atoms. As a consequence neglecting the process of radiation trapping is justified. In this limit the steady-state density distribution is a solution of

$$\gamma n(z,t) - D \frac{\partial^2}{\partial z^2} n(z,t) = S(z). \quad (3)$$

The excitation rate per unit volume $S(z)$ in Eq. (3) is given by Beer's law,

$$S(z) = S_0 \exp[-\alpha(\omega)z], \quad (4)$$

where

$$\alpha(\omega) = \frac{\alpha_0}{1 + (2\Delta\omega/\Gamma_{\text{self}})^2} \quad (5)$$

is the frequency-dependent absorption coefficient of the light in the vapor. Here α_0 is the absorption coefficient at line center, $\Delta\omega = \omega - \omega_0$ the detuning, and Γ_{self} the self-broadened linewidth. Because, for every detuning $\Delta\omega$, all photons that enter the cell are absorbed, the photon flux density Q_0 equals the integrated excitation rate per unit volume i.e.,

$$Q_0 = \int_0^\infty S(z) dz = \frac{S_0}{\alpha}. \quad (6)$$

The general solution to Eq. (3) is given by

$$n(z) = G \exp(-\beta z) + H \exp(\beta z) - \frac{S_0}{D(\alpha^2 - \beta^2)} \exp(-\alpha z), \quad (7)$$

where $\beta = \sqrt{\gamma/D}$ is the inverse of the diffusion length l_τ ; G and H are coefficients that are determined by the boundary conditions. The requirement that the density of excited atoms vanishes at large distances from the entrance window implies that $H=0$. At the entrance window ($z=0$) we have $n(0) \geq 0$ and $dn/dz \geq 0$. The latter condition is equivalent to the statement that the diffusive flow must be directed towards the window. Together, these two boundary conditions for $z=0$ determine an interval of validity for the coefficient G within which all solutions are allowed. Alternatively, one can use the approximate boundary condition [22]

$$0.71l_{\text{re}} \left. \frac{dn}{dz} \right|_{z=0} = n(0). \quad (8)$$

This yields

$$G = \frac{S_0}{D(\alpha^2 - \beta^2)} \left(\frac{1 + 0.71l_{\text{re}}\alpha}{1 + 0.71l_{\text{re}}\beta} \right) \approx \frac{S_0}{D(\alpha^2 - \beta^2)}, \quad (9)$$

where the latter approximation is very well justified in the line core where $l_{\text{re}} \ll \alpha^{-1} < \beta^{-1}$ for sufficiently high densities. For the case where $\alpha \leq \beta$ radiation trapping has to be considered and our model can, therefore, not be applied. In the limit where $\alpha > \beta$ the solution to Eq. (3) is given by

$$n(z) = \frac{S_0}{D(\alpha^2 - \beta^2)} [\exp(-\beta z) - \exp(-\alpha z)]. \quad (10)$$

We measure the total fluorescence F coming from the vapor. Since F is proportional to the total number of excited atoms we integrate the distribution $n(z)$ and using Eq. (6) we find

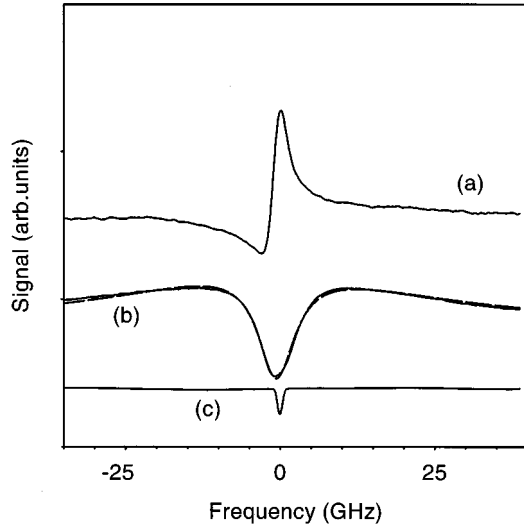


FIG. 2. Reflectivity (a) and fluorescence-excitation (b) spectra on the D_1 line for potassium vapor ($N=0.3 \times 10^{17} \text{ cm}^{-3}$). Curve (c) shows the low-density absorption spectrum. Far off resonance the reflectivity R [curve (a)] has a value of 7.6%, representing the reflectivity of the sapphire-vacuum interface. Around resonance R varies between $R \approx 20\%$ and $R \approx 3\%$. The fluorescence signal [curve (b)] around line center is reduced to 25% of the signal in the line wing.

$$F(\Delta\omega) \propto \int_0^\infty n(z) dz = \left[1 - \frac{\Gamma_{\text{self}}^2 \alpha_0 / \beta}{4\Delta\omega^2 + \Gamma_{\text{self}}^2 (1 + \alpha_0 / \beta)} \right]. \quad (11)$$

The total fluorescence F is seen to display a diplike feature around resonance with a full width at half maximum, width Γ_{dip} ,

$$\Gamma_{\text{dip}} = \Gamma_{\text{self}} (1 + \alpha_0 \sqrt{D/\gamma})^{1/2}. \quad (12)$$

In contrast to the self-broadened width Γ_{self} , which, in the binary collision regime, is strictly proportional to density, Γ_{dip} shows a nontrivial density dependence

$$\Gamma_{\text{dip}}(N) = kN(1 + A/\sqrt{N})^{1/2}, \quad (13)$$

with k the self-broadening coefficient and

$$A = \alpha_0 \sqrt{\frac{DN}{\gamma}} = \alpha_0 \sqrt{\frac{k_B T}{m \langle \sigma_{\text{rev}} \rangle \gamma}}, \quad (14)$$

a density-independent coefficient. It represents the ratio of the diffusion length at unit particle density and the line-center absorption length in the high-density limit (α_0^{-1}).

IV. RESULTS AND DISCUSSION

We have measured the reflection- and fluorescence-excitation spectrum for potassium for densities $N=(0.3-2.5) \times 10^{17} \text{ cm}^{-3}$. Typical results are shown in Figs. 2 and 3 for densities $N=0.3 \times 10^{17}$ and $N=2.0 \times 10^{17} \text{ cm}^{-3}$, respectively.

In both figures curve (c) shows the low-density ($N \approx 10^{11} \text{ cm}^{-3}$) absorption spectrum as measured in a separate cell; it serves as an absolute frequency reference. The reflectivity

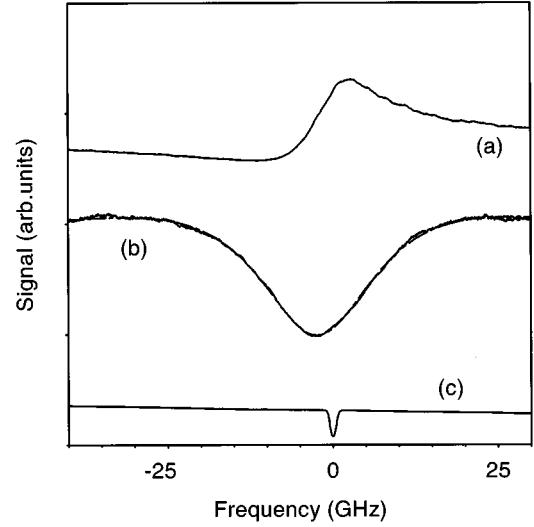


FIG. 3. Reflectivity (a) and fluorescence-excitation (b) spectra on the D_1 line for potassium vapor ($N=2 \times 10^{17} \text{ cm}^{-3}$). Curve (c) shows the low-density absorption spectrum. The fluorescence signal [curve (b)] around line center is reduced to 50% of the signal in the line wing.

tion spectra of the high-density vapor near the sapphire interface are depicted in curves (a). The spectra, offset along the vertical axis, are dispersionlike shaped and centered around the resonance frequency. Curves (b) show the central part of the fluorescence-excitation spectrum. The full excitation spectrum is much broader than the region shown here but the wings do not contain information on the nonradiative effects that we study here. The dashed curves are the results from a fit of the model to the experimental excitation spectrum that will be discussed below.

As shown in Figs. 2 and 3 the frequency-integrated fluorescence output of the excited vapor is strongly reduced when it is excited at line center as compared to the situation where it is excited in the wings of the spectral line. For example, at resonance the fluorescence signal is reduced to 25% for a density $N=0.3 \times 10^{17} \text{ cm}^{-3}$; at a density $N=2 \times 10^{17} \text{ cm}^{-3}$ the signal is reduced to $\approx 50\%$. We attribute the observed reduction of the fluorescence signal around line center to wall collisions of excited atoms (quenching) resulting from diffusive- and nonradiative transport of excitation, as discussed in the Introduction.

Zajonc and Phelps [16] showed that under the conditions prevailing in their experiment the reduction of the fluorescence around resonance is most pronounced if one detects the fluorescence that comes from atoms that have made a fine-structure changing collision. One is sensitive to this class of atoms when one detects the fluorescence on the D_2 line while the laser is tuned to the D_1 line. In order to see whether such a difference between the direct (excitation and detection on the same transition) and sensitized (excitation and detection on different transition) fluorescence also exists under the present experimental conditions we have measured the fluorescence output separately in a band around the D_1 and D_2 transitions, in addition to measuring the total fluorescence. Note that we always excite on the D_1 transition. The results are shown in Fig. 4 for a density $N=1.3 \times 10^{17} \text{ cm}^{-3}$. Curve (b) shows the unfiltered fluorescence while curves (a)

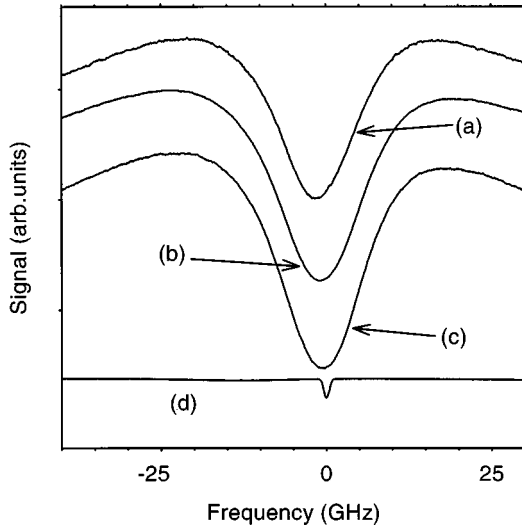


FIG. 4. Fluorescence-excitation spectra or the total fluorescence output (b), the fluorescence measured around the D_1 transition (a), and around the D_2 transition (c). Curve (d) shows the low-density absorption spectrum.

and (c) indicate the fluorescence as detected on the D_1 and D_2 line, respectively. For the sake of clarity the spectra have been given an offset along the vertical axis. The three fluorescence-excitation spectra have very similar shapes with, in all cases, a pronounced dip at line center. The values for the width of the dip in the three cases are equal within a few percent. Therefore, our results, as shown in Fig. 4, justify the use of a two-level description for the transport of excitation in the vapor. Because of the high density in our experiment we may expect, as discussed in the Introduction, to find, even in the line core, a weighted average value for the diffusion coefficient D and the resonance exchange rate coefficient $\langle\sigma_{\text{rev}}\nu\rangle$ for the $P_{1/2}$ and $P_{3/2}$ states.

The fluorescence-excitation spectra of Figs. 2 and 3 are fitted with an expression based on Eq. (11), with two terms added. First, a Lorentzian term has been added in order to account for the radiative transport that determines the fluorescence intensity away from line center. This term gives an adequate description of the shape of the fluorescence excitation spectrum in the radiative limit [10]. Furthermore, a small dispersive term has been added to account for the spectral variation of the transmission of the sapphire-vapor interface due to the dispersive optical response of the vapor. As can be seen from the results shown in Figs. 2 and 3, this description provides an excellent fit to the experimental data around line center. Important parameters that are obtained from the fit are the width and depth of the central dip in the fluorescence-excitation spectrum as well as its center relative to that of the low-density absorption spectrum.

As can be seen in Figs. 2 and 3 the selective reflection- and fluorescence-excitation spectra exhibit a shift of the central frequency with respect to the low-density resonance frequency ω_0 . For the reflection spectrum, this shift, which is linear in density, is usually attributed to a combination of Lorentz local-field shift, collisional shift [5], and wall shift [23]. For the fluorescence-excitation spectrum we find that the line shift, i.e., the central frequency of the dip as compared to ω_0 , is also linear in density; it is likely to originate

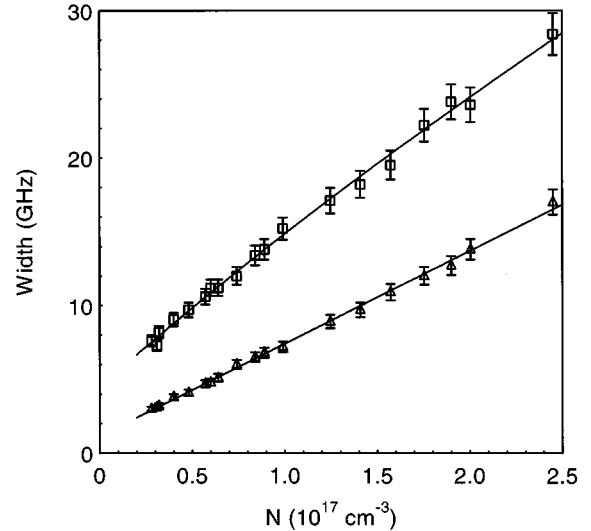


FIG. 5. The width $\Delta\nu_{mm}$ of the selective reflection spectrum (Δ) and the width of the dip in the fluorescence-excitation spectrum (\square) as a function of atomic density N .

from the same sources as the shift in the reflection spectrum.

The results for the width Γ_{dip} (squares) of the central dip in the fluorescence-excitation spectrum as a function of density are shown in Fig. 5. Also shown is the density dependence of the width $\Delta\nu_{mm}$ of the selective-reflection spectrum (triangles); the latter is taken to be the difference between the frequency of maximum reflectivity and that of minimum reflectivity. For a Lorentzian spectral line there exists a relationship between this width $\Delta\nu_{mm}$ and the width of the spectral line; for the D_1 transition one can show that $\Delta\nu_{mm} = 1.15\Gamma_{\text{self}}$ [4], where Γ_{self} is the full width at half maximum of the spectral line. For the density range shown in Fig. 5, the spectral width Γ_{self} is linear in density, as expected. From the slope we find a value for the self-broadening coefficient $k = \Gamma_{\text{self}}/N = \langle\sigma\nu\rangle = 2\pi \times 5.5 \times 10^{-8} \text{ cm}^3 \text{ s}^{-1}$, in reasonable agreement with the results found by Maki *et al.* [4]. The fact that the experimental results for the spectral separation $\Delta\nu_{mm}$ do not extrapolate to zero in the zero density limit is a direct consequence of the fact that we have ignored Doppler broadening and hyperfine structure. One can indeed extract a value for the residual width $\Delta\nu_{\text{res}}$ from the fit to our experimental results. We find $\Delta\nu_{\text{res}} \approx 1 \text{ GHz}$, which is close to the value for the Doppler width at a temperature $T = 700 \text{ K}$ ($N \approx 10^{17} \text{ cm}^{-3}$) combined with the hyperfine splitting of 462 MHz.

Although it is not immediately obvious from the results shown in Fig. 5, the experimental values for Γ_{dip} as a function of density do not fall on a straight line. This is best seen by considering the same results in Fig. 6 where we plot the ratio of Γ_{dip} and Γ_{self} as a function of density. We see a marked nonlinear density dependence of this ratio that is somewhat hidden in Fig. 5 because $\Gamma_{\text{self}} \propto N$. The solid line through the data points is the result of a fit of Eq. (13) to the data; Eq. (13) can be written as

$$\frac{\Gamma_{\text{dip}}}{\Gamma_{\text{self}}} = (1 + \sqrt{N})^{1/2}, \quad (15)$$

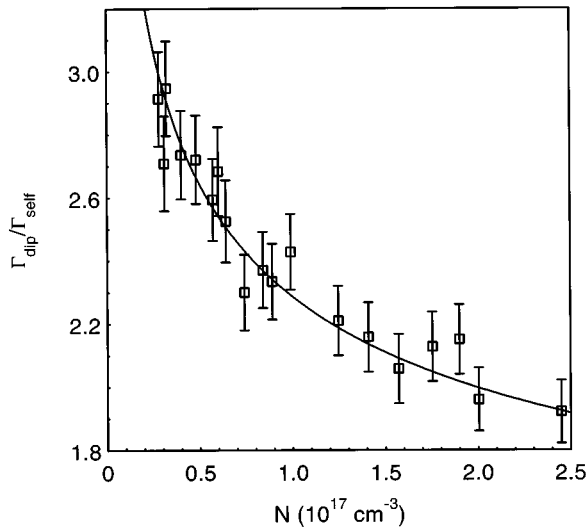


FIG. 6. The ratio of the width Γ_{dip} of the fluorescence dip, and the spectral width Γ_{self} as a function of the atomic density N .

showing the expected density dependence of the ratio that is plotted in Fig. 6. By fitting this equation to the results shown in Fig. 6 or equivalently, the data for Γ_{dip} in Fig. 5 we can extract a value for the density-independent coefficient A . The result is $A = 14.5 \times 10^8 \text{ cm}^{-3/2}$.

From the value of A we can now determine the diffusion coefficient D . For this we need a value for the absorption coefficient at line center and we take $\alpha_0 = 2\pi/\lambda$. Using $\tau = 26 \text{ ns}$ we find $D = 0.05 \text{ cm}^2 \text{ s}^{-1}$ for a density of $N = 1 \times 10^{17} \text{ cm}^{-3}$. Using Eq. (2) for the expression for the diffusion coefficient we extract as value for the resonance-exchange rate coefficient $\langle \sigma_{\text{re}} \nu \rangle = 2\pi \times 2.3 \times 10^{-8} \text{ cm}^3 \text{ s}^{-1}$. When we consider the rate coefficient $\langle \sigma \nu \rangle$ for dipole-dipole collisions irrespective of whether exchange of excitation has occurred or not, with $\langle \sigma \nu \rangle = \Gamma_{\text{self}}/N$, we find that $\langle \sigma \nu \rangle_{D_1} = 2\pi \times 5.5 \times 10^{-8} \text{ cm}^3 \text{ s}^{-1}$. This value is 2.5 times the value for $\langle \sigma_{\text{re}} \nu \rangle$ obtained in the present experiment. This means that roughly every second collision results in an excitation transfer between an excited atom and an atom in the ground state, in good agreement with theoretical models [15]. Note that because of the efficiency of fine-structure mixing our value for $\langle \sigma_{\text{re}} \nu \rangle$ represents an average over the fine-structure states.

For all densities studied we find excellent agreement between our transport model, based on binary collisions, and the experimental data. This implies that the diffusion coefficient D is inversely proportional to density as expected for a binary model. For very high densities it has been suggested that D would become proportional to $N^{1/3}$ [24]. This prediction is based on a model where the atoms are stationary and excitation transfer to neighbor atoms only takes place via ‘‘hopping’’ of excitation. Our results indicate that this behavior is not important at densities $N \leq 3 \times 10^{17} \text{ cm}^{-3}$.

V. CONCLUDING REMARKS

We have experimentally shown that in a dense potassium vapor [$N = (0.3 - 2.5) \times 10^{17} \text{ cm}^{-3}$] the nonradiative transport of excitation is of a diffusive nature. A signature of the nonradiative process is the arisal of a pronounced dip around resonance in the fluorescence-excitation spectrum. The presence of nonradiative transport implies that a fraction of the excitation of the vapor can diffuse to the cell wall and get quenched in a time short or comparable to the excited-state lifetime. This fraction becomes sizable in a high-density vapor with incident laser light tuned to the center of the spectral line.

The presence of nonradiative transport and wall quenching implies that in high-density vapors the optical response of an atomic vapor is affected by spatial inhomogeneities, in particular of the excited-state distribution. The inhomogeneities are especially prominent when the vapor is excited at frequencies in the vicinity of the fundamental resonance frequency. The presence of such inhomogeneities has important implications for experiments where one probes properties of such a dense vapor, in particular when the measurements are done in reflection. One can think here of the apparent lifetime of excited states [18], the line shape of multiphoton transitions [25], and nonlinear optical effects such as electromagnetically induced transparency [26].

ACKNOWLEDGMENTS

We gratefully acknowledge C. J. C. Smeets for help with the experiments. This work is part of the research program of the ‘‘Stitching voor Fundamenteel Onderzoek der Materie’’ and was made possible by the financial support from the ‘‘Nederlandse Organisatie voor Wetenschappelijk Onderzoek.’’

-
- [1] J. A. Leegwater and S. Mukamel, *Phys. Rev. A* **49**, 146 (1994).
 - [2] R. Friedberg, S. R. Hartmann, and J. T. Manassah, *Phys. Rep.* **7**, 101 (1973); *Phys. Rev. A* **39**, 3444 (1989); **40**, 2446 (1989); **42**, 5573 (1990).
 - [3] F. A. Hopf, C. M. Bowden, and W. H. Louisell, *Phys. Rev. A* **29**, 2591 (1984).
 - [4] J. J. Maki, M. S. Malcuit, J. E. Sipe, and R. W. Boyd, *Phys. Rev. Lett.* **67**, 972 (1991).
 - [5] J. J. Maki, W. V. Davis, R. W. Boyd, and J. E. Sipe, *Phys. Rev. A* **46**, 7155 (1992).
 - [6] A. S. Manka, J. P. Dowling, C. M. Bowden, and M. Fleischer, *Quantum Opt.* **6**, 371 (1994).
 - [7] Y. Ben-Aryeh, C. M. Bowden, and J. C. Englund, *Phys. Rev. A* **34**, 3917 (1986).
 - [8] M. P. Hehlen, H. U. Güdel, Q. Shu, J. Rai, S. Rai, and S. C. Rand, *Phys. Rev. Lett.* **73**, 1103 (1994).
 - [9] C. R. Stroud and C. M. Bowden, *Opt. Commun.* **67**, 387 (1988).
 - [10] T. Holstein, *Phys. Rev.* **83**, 1159 (1951).
 - [11] G. Van Volkenburgh and T. Carrington, *J. Quant. Spectrosc. Radiat. Transf.* **11**, 1181 (1971).
 - [12] W. Molander, M. Belsley, A. Streater, and K. Burnett, *Phys. Rev. A* **29**, 1548 (1984).

- [13] W. R. Hindmarsh, *Atomic Spectra* (Pergamon, Oxford, 1967).
- [14] R. G. Fowler, in *Handbuch der Physik* Vol. 22 (Springer-Verlag, Berlin, 1956), p. 226.
- [15] A. V. Phelps and A. O. McCoubrey, *Phys. Rev.* **118**, 1561 (1960).
- [16] A. G. Zajonc and A. V. Phelps, *Phys. Rev. A* **23**, 2479 (1981).
- [17] T. Fujimoto and A. V. Phelps, *Phys. Rev. A* **25**, 322 (1982).
- [18] V. A. Sautenkov, R. G. Gamidov, and A. Weis, *Phys. Rev. A* **55**, 3137 (1997).
- [19] J. P. Woerdman and M. F. H. Schuurmans, *Opt. Commun.* **16**, 248 (1975).
- [20] E. L. Lewis, *Phys. Rep.* **58**, 1 (1980).
- [21] A. F. Molisch, B. P. Oehry, W. Schupita, B. Sumetsberger, and G. Magerl, *J. Quant. Spectrosc. Radiat. Transf.* **52**, 841 (1994).
- [22] P. M. Morse and H. Feshbach, *Methods of Theoretical Physics* (McGraw-Hill, New York, 1953).
- [23] J. Guo, J. Cooper, and A. Gallagher, *Phys. Rev. A* **53**, 1130 (1996).
- [24] A. V. Phelps and C. L. Chen, *Bull. Am. Phys. Soc.* **15**, 428 (1970).
- [25] H. van Kampen, V. A. Sautenkov, E. R. Eliel, and J. P. Woerdman (unpublished).
- [26] K.-J. Boller, A. Immamoğlu, and S. E. Harris, *Phys. Rev. Lett.* **66**, 2593 (1991).